

## **General Disclaimer**

### **One or more of the Following Statements may affect this Document**

- This document has been reproduced from the best copy furnished by the organizational source. It is being released in the interest of making available as much information as possible.
- This document may contain data, which exceeds the sheet parameters. It was furnished in this condition by the organizational source and is the best copy available.
- This document may contain tone-on-tone or color graphs, charts and/or pictures, which have been reproduced in black and white.
- This document is paginated as submitted by the original source.
- Portions of this document are not fully legible due to the historical nature of some of the material. However, it is the best reproduction available from the original submission.

(NASA-CR-175329) A MERCURIC DETECTOR SYSTEM  
FOR X-RAY ASTRONOMY. 2. RESULTS FROM  
FLIGHT TESTS OF A BALLOON BORNE INSTRUMENT  
(Massachusetts Inst. of Tech.) 30 p  
HC A03/MF A01

N84-16095

Unclass

CSCD 03A G3/89 11383

A MERCURIC DETECTOR SYSTEM FOR X-RAY ASTRONOMY:  
II. RESULTS FROM FLIGHT TESTS OF A BALLOON BORNE INSTRUMENT<sup>1</sup>

J.V. Vallerger, R.K. Vanderspek, and G.R. Ricker

Center for Space Research  
Massachusetts Institute of Technology  
Cambridge, MA 02139

CSR-HEA-82-46

ABSTRACT

To establish the expected sensitivity of a new hard X-ray telescope design, described in Ricker, Vallerger and Wood (Paper I), an experiment was conducted to measure the background counting rate at balloon altitudes (40 km) of mercuric iodide, a room temperature solid state X-ray detector. The prototype detector consisted of two thin mercuric iodide ( $\text{HgI}_2$ ) detectors surrounded by a large bismuth germanate ( $\text{Bi}_4\text{Ge}_3\text{O}_{12}$ ) scintillator operated in anticoincidence. The bismuth germanate shield<sup>3</sup> vetoed most of the background counting rate induced by atmospheric gamma-rays, neutrons and cosmic rays.

A balloon-borne gondola containing a prototype detector assembly was designed, constructed and flown twice in the spring of 1982 from Palestine, Texas. The second flight of this instrument established a differential background counting rate of  $4.2 \pm 0.7 \times 10^{-2}$  counts/sec  $\text{cm}^2$  keV over the energy range of 40 to 80 keV. This measurement was within 50% of the predicted value. The measured rate is 5 times lower than previously achieved in shielded NaI/CsI or Ge systems operating in the same energy range. The prediction was based on a Monte Carlo simulation of the detector assembly in the radiation environment at float altitude. Details of the simulation can be found in Paper I.

<sup>1</sup>This work is supported in part by NASA grants NSG-7339 and NAGW-14.

## 1.0 INTRODUCTION

In order to test and confirm detector models used in the previous paper (paper I), a small balloon-borne gondola containing a prototype detector for a hard X-ray diffraction telescope was designed, constructed and flown at balloon altitudes. Its purpose was to measure the background counting rate at the eventual telescope operating environment ( $>40$  km altitude, balloon or satellite). The radiation environment (X- and gamma rays, high energy charged particles, neutrons) at high altitude is quite different from that at sea level. Atmospheric shielding and ground radiation have much greater effects near sea level. In this paper, the measurements at high altitude are compared with predictions made by a detector Monte Carlo simulation (paper I). Once the simulation is checked, the design parameters (geometry of detectors, shielding components and discriminator settings) can be varied in the simulation to optimize (lower) the expected background counting rate.

The small gondola used in these experiments can be conceptually divided into two subsystems: the prototype detector consisting of a bismuth germanate shielded mercuric iodide detector (paper I, fig. 2) described in Section 2; and the detector support systems consisting of electronics, power systems, and data recording, all described in Section 3. Section 4 gives the results of the background measurements at sea level and at balloon altitudes.

## 2.0 Prototype Detector System

The overall design goal for the Hard X-ray Diffraction Telescope (HXDT) described in Paper I is to minimize the number of background events in the energy range of 40-80 keV while keeping the response to concentrated signal X-rays as high as possible. The proposed concentrator requires a detector with an area approximately equal to the size of its focal "spot" ( $\sim 1 \text{ cm}^2$  for a lithium fluoride concentrator optimized for 40-80 keV). The detector must

also have a field of view larger than the solid angle subtended by the concentrator to "see" all diffracted signal X-rays ( $\Omega \sim .12$  steradian for the HXDT concentrator). The active anticoincidence shield should surround the entire detector except for the entrance aperture to be most effective at vetoing non-aperture radiation. Passive mass viewed by the detector (e.g., structural material such as aluminum) should be minimized because secondary radiation generated in this mass might not be vetoed.

The prototype detector system consists of two  $\text{HgI}_2$  detectors mounted back to back and operated in anticoincidence. The two detectors are placed inside a bismuth germanate ( $\text{Bi}_4\text{Ge}_3\text{O}_{12}$  or "BGO") scintillating shield along with two hybrid charge sensitive preamps. The BGO shield is also operated in anticoincidence with the main (top) detector. The axially symmetric "well" containing the detectors is gas-tight (.5mm Al entrance window) to retain a pressure of one atmosphere at balloon altitudes. Such a gas-tight enclosure eliminates the problem of high voltage corona breakdown encountered at low atmospheric pressures and avoids the need for potting the detector assembly.

## 2.1 Primary Mercuric Iodide Detector

The "main"  $\text{HgI}_2$  detector that will eventually be used to detect X-rays from a celestial X-ray source is the top detector in the back to back geometry (Fig. 1). The  $\text{HgI}_2$  detector used in the test flights has an effective area of  $0.8 \text{ cm}^2$  (defined by the size of the palladium electrode) and is 390 microns thick. The bottom detector has the same area and is ~1000 microns thick. The bottom detector's main purpose is to provide active shielding from radiation generated in the passive material underneath (printed circuit boards and preamps) as well as better protection from aperture charged particle flux. The  $\text{HgI}_2$  detectors are separated by a thin (13 $\mu\text{m}$ ) mylar insulator and mounted on a Rexolite substrate. The  $\text{HgI}_2$  crystals are grown and then fabricated into

the "back to back" units by EG&G, Inc., Santa Barbara.

The charge sensitive preamps are mounted on paper based printed circuit boards and are held in place underneath the bottom detector by a low mass stainless steel structure. A glass epoxy lased printed circuit board was avoided because of the high concentration of potassium 40 in natural glass (ref. 1, pg. 775). The preamps were based on a low power design used for the SAS-C X-ray Satellite<sup>2</sup> and were modified and hybridized by EG&G, Las Vegas. They were placed close to the detectors to minimize input capacitance and noise pickup. These compact, self-contained preamps were chosen because of their proven reliability and availability. In future designs we will consider placing only the input field effect transistor (FET) in the well to reduce the passive mass. Small copper wires bring preamp power, high voltage, and ground connections down into the well to the detector assembly and the top and bottom detector signals out of the well. The well is lined with electrically grounded aluminum (.25 mm thick) to provide electromagnetic shielding. RC filters for the high voltage and preamp power are mounted outside the well and the field of view of the detectors but inside the pressure container.

## 2.2 Bismuth Germanate Shield

Bismuth germanate was chosen as the shield material because of its very high photoelectric cross section and density.<sup>3</sup> In terms of its stopping power it can almost be considered "active lead". The crystal is 7.5 cm in diameter and 12.5 cm long with a machined 7.4 cm deep x 2.5 cm diameter axially symmetric well in which the  $\text{HgI}_2$  detectors are placed. The outside surface of the crystal is coated with reflective paint and encased in aluminum to protect the crystal and prevent light leaks. A Hamamatsu R1307 photomultiplier is mounted on the unpainted bottom of the BGO crystal opposite the well (paper I, fig. 2) and surrounded by a mu metal shield to protect it from magnetic field

induced gain changes.

At the time when the BGO was ordered from Harshaw Chemical Co., the 7.5 cm diameter was the largest size available. The 2.5 cm inner diameter of the well was determined by the preamp size and ease of construction. In the energy range where BGO has the smallest attenuation coefficient ( $\sim 1$  to 3 MeV), non-aperture gamma rays that intersect the  $\text{HgI}_2$  must traverse at least 2.5 cm of BGO ( $\sim 1$  attenuation length). At lower and higher energies the attenuation is much greater. The top  $\text{HgI}_2$  detector is placed 2.6 cm deep into the well measured from the top of the BGO. The BGO then acts as the collimator with a flat topped response and an effective circular field of view of  $\sim .12$  steradians.

With such a large field of view the diffuse atmospheric and cosmic X-ray background would dominate the background count rate. For the diffracting concentrator concept to work, X-rays that can reach the  $\text{HgI}_2$  detector directly through the aperture must be stopped so that only diffracted X-rays from a celestial X-ray source are detected. The "direct" (undiffracted) field of view must be blocked using a graded shield of lead, tungsten, and tin. The lower atomic number materials are included to stop the characteristic K X-rays of the higher. For the test flight of the prototype detector this passive shield was placed directly over the entrance window though in actual use with a concentrator it would be further from the detector so as not to block the diffracted X-rays. This is shown schematically in Fig. 2. The transmission of 1 mm of Pb + 1 mm of W + 2.5 mm of Sn is shown in Fig. 3.

### 3.0 Balloon Gondola and Associated Electronics

The detector prototype (BGO shield and  $\text{HgI}_2$  detectors) is contained in a small (30 cm x 30 cm x 45 cm) aluminum framed package along with its support electronics. Power for the electronics and heaters is supplied by lithium

batteries while the high voltage for the  $\text{HgI}_2$  crystals comes from a charged 0.2 microfarad capacitor. The capacitor stays within 30% of its original voltage for ~30 hours because of the small leakage currents of the detectors, cables, and the capacitors themselves. The capacitor is fully charged just before launch. This simple detector biasing method provides lower noise levels than does a low-to-high voltage converter. Low voltage experiment power is turned on at approximately 6 km altitude by parallel pressure switches operating a relay. This conserves the batteries and protects against electrical shorting at launch and landing.

Once power is turned on in flight, data collection begins. The main part of the electronics takes random, asynchronous voltage pulses from the detector preamp, converts these pulses into synchronous, 8 bit digital words and routes these words to an appropriate magnetic tape track. The remainder of the electronics monitors the condition of the gondola (temperatures, voltages, currents, etc.) and records this housekeeping data on a separate magnetic tape track. The gondola is self contained during flight (i.e., no telemetry, no commands, no interface). However, it is essential that the cassette tape be recovered!

### 3.1 Event Logic Electronics

Pulse height spectra are recorded for both top and bottom  $\text{HgI}_2$  detectors. Output pulses from the BGO photomultiplier are fed into an Amptek A-101 logarithmic amplifier/discriminator which produces a digital pulse if the charge pulse amplitude is above a set threshold. For the BGO shield, only the integral count rate is recorded; no pulse height information is retained.

Small voltage pulses from both  $\text{HgI}_2$  detector preamps are brought to pulse shaping voltage amplifiers (time constant ~15 $\mu$ s). The last stage of these amplifiers is a "peak stretcher" which retains the maximum voltage attained by

the pulse and holds it at the input of an analog to digital converter until reset. If the pulse height triggers the lower level discriminator, the pulse height will be converted 22  $\mu$ seconds later to an 8 bit digital word. For the top  $\text{HgI}_2$  detector, the event logic determines if an event occurred in the BGO crystal or the bottom detector in the time interval from 13  $\mu$ s before the top event to 9  $\mu$ s after. If no "veto" event occurs during this interval, then the 8 bit digital word is shifted to the "valid" buffer for tape track #1. If a "veto" event occurs in either the BGO or the bottom crystal then the 8 bit word is shifted into the "veto" buffer for tape track #2. All events occurring in the bottom crystal are converted and shifted into the "bottom" buffer for tape track #3. Once the shift into the buffer takes place, the peak stretcher is reset and ready for a new pulse. Total time from event to reset is approximately 50 microseconds. The event logic diagram is shown in Fig. 4.

Because of the very low count rates in the  $\text{HgI}_2$  detectors at float ( $\sim 1$  ct/sec) the dead times due to the finite conversion time are negligible. The BGO count rate of  $\sim 1000$  cts/sec plus the veto flag duration of 22 microseconds gives a 2% probability that a valid event will be vetoed by accident.

#### 4.0 RESULTS OF BACKGROUND MEASUREMENTS AT SEA LEVEL AND AT BALLOON ALTITUDES

##### 4.1 Sea Level Background

The radiation environment on the ground consists mostly of high energy gamma rays due to the decay of naturally occurring radioactive isotopes such as potassium 40 and uranium and thorium daughter products. Primary cosmic rays and neutrons are shielded by the atmosphere but secondary muons do reach ground level. The gamma ray intensity is a strong function of the type of



building where the measurements take place. Wood frame buildings are usually less active than concrete buildings due to the amount of radionuclides in sand and cement.

Long term background spectra were accumulated with the prototype detector gondola in many locations and many configurations. Fig. 5 shows the normalized count rates for spectra obtained in: Building 37, 5th floor, MIT; a ground floor preparation room at the National Scientific Balloon Facility in Palestine, Texas; and the iron cave in the basement of Building 2 at MIT. Integrated count rates are compared in Table 1 along with the BGO shield count rate. The iron cave results provide an upper limit to the intrinsic background of the prototype detector (background due to radioactive material used in the construction of the detector assembly itself) though extrinsic muons are more likely to be the cause of this background. The gamma ray contribution can be scaled with the bismuth K line observed in the veto spectrum. The veto ratio (the number of vetoed counts divided by the total counts) increased in the iron cave as the bismuth line decreased. This would be expected if the iron cave background is dominated by charged muons.

The effectiveness of the various shielding systems is shown in Fig. 6 where the  $\text{HgI}_2$  valid spectra are shown with the BGO shield off and the bottom  $\text{HgI}_2$  crystal off. The BGO shield does provide most vetoes, especially vetoing the K line of bismuth as expected. The bottom  $\text{HgI}_2$  does decrease the integrated count rate by another factor of  $\sim 2$  in the range of 40-80 keV.

#### 4.2 Energy Calibration

The 8 bit pulse height analyzer (0-255) was calibrated using gamma rays from radioactive sources such as  $^{145}\text{Pm}$  (37 keV),  $^{241}\text{Am}$  (59.5 keV) and  $^{57}\text{Co}$  (122 keV). Unlike photomultipliers, solid state detectors are not strongly affected by small changes in the bias voltage. The peak position of the  $^{241}\text{Am}$

60 keV line feature moved less than one channel as the detector bias was decreased from 300 volts to 200 volts, a drop expected in a 30 hour balloon flight. An in-flight calibration source was not included on the gondola because of this gain stability plus the fact that the bismuth K X-ray calibration is already "built in" due to fluorescence of the BGO shield.

The voltage amplifier gain was adjusted to place the 59.5 keV line approximately near channel 60 (in actuality channel 57, see Fig. 7). The dynamic range then was from 15 keV to 265 keV, with all larger events ending up in channel 255. The voltage amplifier was modified before the second flight to give an approximately logarithmic gain above 120 keV though it remained linear below an energy of 120 keV. The complete dynamic range extended from 10 keV to 670 keV.

The detector used for flight has a resolution of 5.5 keV at 60 keV so the quantization error of one channel/keV was negligible. This detector was chosen for its stability and size and was operated at only 300 volts to decrease leakage current "bursts" that mimic background counts. Some energy resolution was sacrificed since the dominant background contributors of interest produce a continuum of counts vs. energy.

#### 4.3 Balloon Flights

The small prototype detector gondola was flown twice from Palestine, Texas. The first time, flight 1282P, was a "piggyback" flight in which the small gondola was strapped on the side of a large (1400 kgs.) payload flown by Martin Israel's group at Washington University, St. Louis. The first flight was launched at 12:25 UT, May 8, 1982. It reached float altitude at 14:48 UT at an altitude of 38 km ( $3.8 \text{ gm/cm}^2$  vertical atmospheric column density). The flight lasted 35.5 hours and was successfully recovered in Mississippi. Analysis of the housekeeping data showed that the batteries began to fail

after 13 hours, probably due to a defective lithium cell since they were expected to last 35 hours.

Another problem observed in the first flight was multiple triggering on energetic events due to extreme saturation of the voltage amplifier. The extra events had a characteristic signature of preferentially occurring with a channel number of 4N-1. This effect was duplicated in the laboratory by applying large pulses to the input of the voltage amplifier as would have occurred during flight if a very energetic particle interacted in the detector. This was a small effect in the veto and bottom detector spectra but it dominated the valid spectrum, increasing the count rate by a factor of 5. Two modifications were made to the electronics. Diodes were placed at the input and on the feedback loops of the voltage amplifier so that large pulses from the preamps would only slightly saturate the last stage. In addition, a time constant was changed in the event logic so that the analog to digital converter would not accept another pulse for 750 $\mu$ sec after it converted a pulse. Despite this lock-out period, the additional dead time was negligible (.07% for a count rate of ~1 ct/sec). The change in the voltage amplifier required a new energy calibration (see above).

The second flight, 1296P, was a solo flight for the small gondola using a small ( $62 \times 10^3$  m<sup>3</sup>) balloon. The launch was at 12:00 UT on June 21, 1982 and a float altitude of 40.2 km (2.8 gm/cm<sup>2</sup> vertical atmospheric column density) was reached at 14:01 UT. The successful 7 hour flight was terminated at 21:00 UT and reached ground 43 minutes later ~60 km Northwest of Pecos, Texas. The payload struck a 130,000 volt power line, resulting in the parachute being ripped apart and the payload free-falling the last 15 meters. Although its styrofoam thermal cover burned on the outside, the payload received only minor mechanical damage and the data tape was recovered intact. The free fall also

demonstrated the ruggedness of the BGO shield which operated flawlessly upon its return to the laboratory.

#### 4.4 Flight Results and Comparison to Predictions

The background spectra of flight 1282P for both  $\text{HgI}_2$  detectors, top and bottom, are shown in Fig. 8. Only the vetoed spectrum of the top detector is presented because the valid spectrum was contaminated with spurious events due to multiple triggering of the event logic by energetic particles. The spectra from flight 1292P are presented in Figs. 9 and 10. The electronic modifications made between flights were successful in suppressing the multiple triggering and the valid spectrum (Fig 10) is free of the single channel peaks.

All these spectra were integrated over time starting at float and ending at flight termination (or power failure for flight 1282P). Arrival at float altitude coincided with a leveling off of the count rate versus time, as shown in Fig. 11. The two maxima in the count rate vs. time plot are due to the Pfozter maximum, the altitude (~17 km.) at which the flux of cosmic ray secondaries reaches its peak. The payload passed through this region slowly on the way up and quickly on the way down.

The vetoed spectra for both flights are very similar in that they are featureless except for the bismuth and possibly mercury K X-ray line features. The K beta X-ray of bismuth was resolved in the second flight. The overall count rate at float decreased by about 25 to 35% from the first flight to the second. This occurred in both detectors, top and bottom. Changes this large cannot be explained by the differences in altitude between the two flights. To interpret this difference as being due to the altitude dependence of the background would require that the float altitudes of the two flights be different by ~6 km, when, in actuality, they only differed in altitude by 2 km. The only other differences between the two flights was the change in the event

logic electronics and the absence of the adjacent 1400 kg. payload in the second flight. Multiple triggering only accounted for a small part of the higher count rate in the first flight based on the number of events in the single channel peaks (see Section 4.3). A massive payload above the detector as in flight 1282P, however, would produce an increase in the local radiation flux due to interactions with the primary cosmic rays. If the massive payload is responsible for the higher count rate in the first flight it would be equivalent to an atmospheric slab of  $9 \text{ gm/cm}^2$  vertical column density.

As expected, the total number of valid background counts accumulated during the second flight was small (31 counts, 40 to 80 keV) and the spectrum is featureless. There are a few extra counts (6 counts total) close to 59 keV. For a flight of this duration, 2.6 counts would be expected at this energy from inelastic neutron scattering from the  $^{127}\text{I}$  nucleus.

Unfortunately, the tungsten K-alpha X-ray energy is also 59 keV so this barely significant feature might also be fluorescence of the passive graded shield or a combination of both. Based on their timing signature (many simultaneous low energy events), the excess number of counts at very low energies ( $< 20 \text{ keV}$ ) were found to be due to leakage current "bursts".

Table 2 contains the float background count rate predictions of Paper I as well as the measured values. The valid count rate agrees surprisingly well. The gamma ray prediction of the Monte Carlo simulation<sup>4</sup> can be directly tested against the strengths of the K alpha and beta line features of mercury and bismuth in the vetoed spectrum. During flight 1292P, the measured value was 25% smaller than predicted, which might indicate that the gamma ray contribution was overestimated. This is also indicated in the energies above 160 keV. If the gamma ray prediction is scaled down to match the measured results for the line features and the higher energies then the discrepancy at

lower energies would be enhanced. This discrepancy probably indicates that the neutron contributions at lower energies were underestimated, which could easily be the case, considering the uncertainties in the neutron fluxes and cross sections.

## 5.0 CONCLUSIONS

Previous to the research work described in these papers, it had been conjectured that  $\text{HgI}_2$  might have great potential for use in hard X-ray astronomy. The combination of high energy resolution at room temperature plus a high photon quantum efficiency seemed ideal for many balloon and satellite detector applications. Yet, experience in field operations with  $\text{HgI}_2$  was minimal<sup>6</sup> and background count rate information obtained with an optimized system at high altitudes did not exist. Development of  $\text{HgI}_2$  specifically for use as an astronomical X-ray detector over the last 3 years has changed this situation (refs. 5,6,7,8). Procedures for handling and packaging detectors have been developed that produce stable and dependable  $\text{HgI}_2$  detectors for use in the field.  $\text{HgI}_2$  detector assemblies have been constructed and flown at balloon altitudes and the detectors operated flawlessly on all occasions.

A major limitation to the application of  $\text{HgI}_2$  in X-ray astronomy is the inability to fabricate individual detectors larger than  $\sim 1 \text{ cm}^2$ . A scheme to overcome this limitation involves the use of X-ray concentrators to increase the effective area of a shielded, low-background  $\text{HgI}_2$  detector, (the HXDT; see Paper I). The concentrator consists of a paraboloid shell lined with lithium fluoride crystals that Bragg diffract on-axis incoming X-rays to the focus of the paraboloid, where a small area detector is located. To establish the expected sensitivity of this concentrator/detector design, the background counting rate of the shielded  $\text{HgI}_2$  detector at balloon altitudes had to be determined.

A balloon-borne gondola containing a prototype detector assembly was designed and constructed to measure this background rate. This gondola was flown twice in the spring of 1982 from Palestine, Texas. The second flight of this prototype instrument established a background counting rate for a bismuth germanate-shielded mercuric iodide detector of  $4.2 \pm 0.7 \times 10^{-5}$  counts/sec cm<sup>2</sup> keV over the energy range of 40-80 keV. This measurement was within 50% of the predicted value. The measured rate is ~5 times lower than previously found with shielded NaI/CsI or Ge systems operating in the same energy range. The prediction was based on a Monte Carlo simulation of the detector assembly in the radiation environment at float altitude (~40km). The Monte Carlo simulation can now be used to investigate the detector design parameters (geometry, discriminator levels, etc.) to attempt to lower the background rate even further.

Based on a background rate of  $4.2 \times 10^{-5}$  cts/sec cm<sup>2</sup> keV, calculations indicate that with 4 concentrators and 4 detectors systems a celestial X-ray source with 1/100 the intensity of the Crab Nebula could be detected in 1.5 hours. This excellent sensitivity is achieved by simultaneously reducing the background by shielding a HgI<sub>2</sub> detector with BGO, and by increasing the effective area using hard X-ray concentrators.

The prescription for reducing the background rate by a factor of ~10 over previous balloon-borne hard X-ray detectors can be summarized very simply: use very high quantum efficiency detectors shielded by dense, high Z active scintillators. Because they are well suited to this experimental approach, HgI<sub>2</sub> and BGO are both likely to become major detector materials in X-ray astronomy. Furthermore, their ease of handling and improved performance at moderately reduced temperatures<sup>7</sup> enhance their desirability for balloon and satellite use.

## ACKNOWLEDGEMENTS

The authors wish to thank: Robert Kubara and the launch crew at the National Scientific Balloon Facility for two highly successful balloon flights; Wayne Schnepple, Carol Ortale and John Warren at EG & G, Santa Barbara for assistance in crystal selection and testing; Andrezj Dabrowski at the Medical Imaging Group, U.S.C. for numerous helpful discussions. Marv Israel kindly provided a "hitchhike" flight opportunity (flight 1282P). At the Center for Space Research at MIT, we wish to thank John Doty, Bob Goeke, Dan Griscon, John Kruper and Pete Tappan for assistance at every stage of gondola design, construction, and testing. This work is supported in part by NASA grants NSG-7339 and NAGW-14.



## REFERENCES

1. Knoll, G.F. 1979, Radiation Detection and Measurement (Wiley & Sons: New York).
2. Goeke, R. 1975, IEEE Trans. on Nucl. Sci., NS-22, 600.
3. Farukhi, M.R. 1978, Technical Paper No. TP16 REVA 0679, Harshaw Chemical Co., Solon, Ohio.
4. Wood, D.R. 1982, "Effects of Atmospheric Gamma Rays on the Background of a Bismuth Germanate-Shielded Mercuric Iodide Detector: A Monte Carlo Analysis", Senior thesis, MIT.
5. Vallergera, J.V., Ricker, G.R., Schnepple, W. and Ortale, C., 1982, I.E.E.E. Trans. on Nucl. Sci., NS-29, No. 1. p.151
6. Ogawara, Y., Mitsuda, K., Vallergera, J.V., Cominsky, L., Kruper, J., Grunsfeld, J., Ricker, G.R., 1982, Nature, 295, p. 675
7. Ricker, G.R., Vallergera, J.V., Dabrowski, A., Entine, G., 1982, Rev. of Sci. Inst., 53, No. 5, p. 700
8. Vallergera, J.V., 1982, "Studies of New Hard X-ray Detection Methods and Observations of Cosmic X-ray Sources", Ph.D. Thesis, M.I.T.

Table 1

Measured Background Count Rate of BGO-Shielded  
Top  $\text{HgI}_2$  Detector for Various Surface Locations

<u>Location</u>	<u>Valid Count Rate<sub>2</sub> (40-80keV)</u> <u>(cts/sec cm<sup>2</sup> keV)</u>	<u>Veto<sup>†</sup></u> <u>Ratio</u>	<u>Bismuth<sup>††</sup></u> <u>K X-ray</u>	<u>BGO</u> <u>Count Rate</u>
Balloon Lab MIT Bldg. 37	$1.8 \times 10^{-5}$	91%	$14 \times 10^{-4}$	1231 cts/sec
Balloon Base Palestine, Tx.	$1.0 \times 10^{-5}$	89%	$5 \times 10^{-4}$	791 cts/sec
Iron Cave MIT Bldg. 2	$.2 \times 10^{-5}$	94%	$1 \times 10^{-4}$	527 cts/sec

† Ratio of number of vetoed counts to total counts (veto + valid)  
over the energy range 40-160 keV

†† Counts/sec cm<sup>2</sup> observed in the vetoed spectrum

Table 2

Comparison of Measured and Predicted Count Rates at Float  
in the Top  $\text{HgI}_2$  Detector for Flight 1292P

<u>Energy (keV)</u>	<u>Valid Count Rate (<math>10^{-5}</math> cts/sec <math>\text{cm}^2</math> keV)</u>	
	<u>Predicted<sup>†</sup></u>	<u>Measured</u>
40 - 80	2.9	$4.2 \pm .7$
80 -120	1.6	$2.6 \pm .6$
120-160	1.0	$1.9 \pm .5$
160-200	1.8	$1.5 \pm .5$
200-240	1.7	$1.0 \pm .4$

Bismuth and Mercury K X-ray line feature<sup>††</sup>:

<u>Predicted<sup>†</sup></u>	<u>Measured</u>
$3.6 \times 10^{-2}$ cts/sec $\text{cm}^2$	$2.7 \times 10^{-2}$ cts/sec $\text{cm}^2$

† Sum of predicted background due to gamma rays and neutrons  
(See paper I). The gamma ray contribution was determined by a Monte Carlo simulation while the neutron contribution was calculated analytically.

†† Present only in vetoed spectrum

Figure captions for Paper II:

- Figure 1 Detailed view of mercuric iodide detector assembly showing the components that fit in the axially symmetric well inside the bismuth germanate shield.
- Figure 2 Schematic of the diffraction concentrator showing the passive graded shields (lead, tungsten, and tin) stopping background aperture X-rays that would normally impinge on the mercuric iodide detector. Only on-axis X-rays that are diffracted by the concentrator reach the detector.
- Figure 3 Transmission of photons vs. energy through a graded shield of 1mm of lead, 1 mm of tungsten and 2.5 mm of tin. The lower Z metals act to stop the fluoresced K X-rays of the higher Z metals.
- Figure 5 Sea level valid background spectra in top mercuric iodide detector for various experiment sites.
- Figure 6 Valid background spectra in top mercuric iodide detector showing the effectiveness of the anticoincidence shields.
- Figure 7 Actual mercuric iodide flight detector calibration spectrum using a  $^{241}\text{Am}$  radioactive source. The energy resolution at 300V (flight bias) was 5.5 keV FWHM at 60 keV.
- Figure 8 Vetoed and bottom spectra from flight 1282P. The veto rate of the top detector was .15 counts/sec over the energy range 40 to 80 keV. As can be seen, the energy resolution of the bottom detector (used as an anticoincidence shield) was substantially broader than the top detector.
- Figure 9 Vetoed and bottom spectra from flight 1292P. Note the decrease in count rate from the previous flight as well as the resolved bismuth K-beta X-ray at 87 keV in the vetoed spectrum.
- Figure 10 Valid spectrum from flight 1292P. The measured background rate was  $4.2 \times 10^{-5}$  counts/sec  $\text{cm}^2$  keV (40-80 keV). There is a possible feature at 59 keV (see text). The increase in count rate below the 40-80 keV range of interest was due to detector leakage current "bursts" (see text).
- Figure 11 Count rate vs. time of the bottom detector during flight 1292P showing both ascending and descending passages through the Pfotzer maximum and the steady count rate at float altitude.

ORIGINAL PAGE IS  
OF POOR QUALITY

## HgI<sub>2</sub> DETECTOR ASSEMBLY (DETAIL)

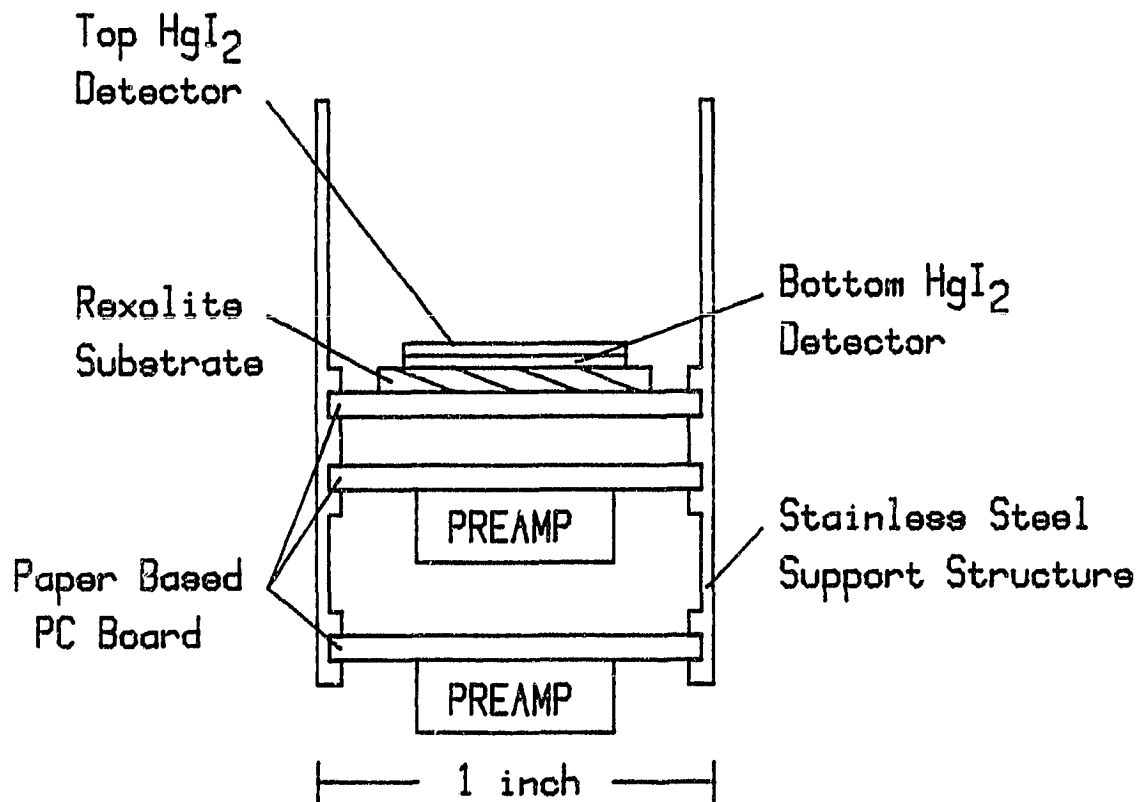


FIGURE 1

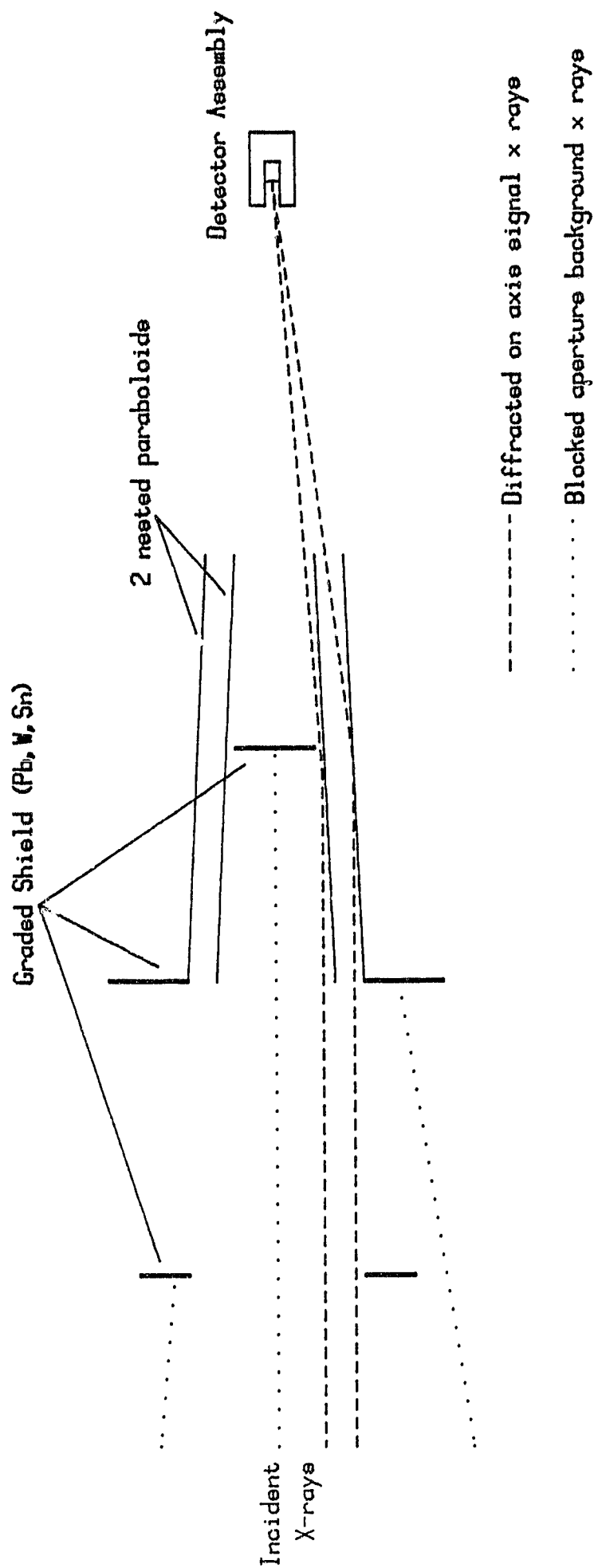


FIGURE 2

ORIGINAL PAGE IS  
OF POOR QUALITY

ORIGINAL PAGE 18  
OF POOR QUALITY

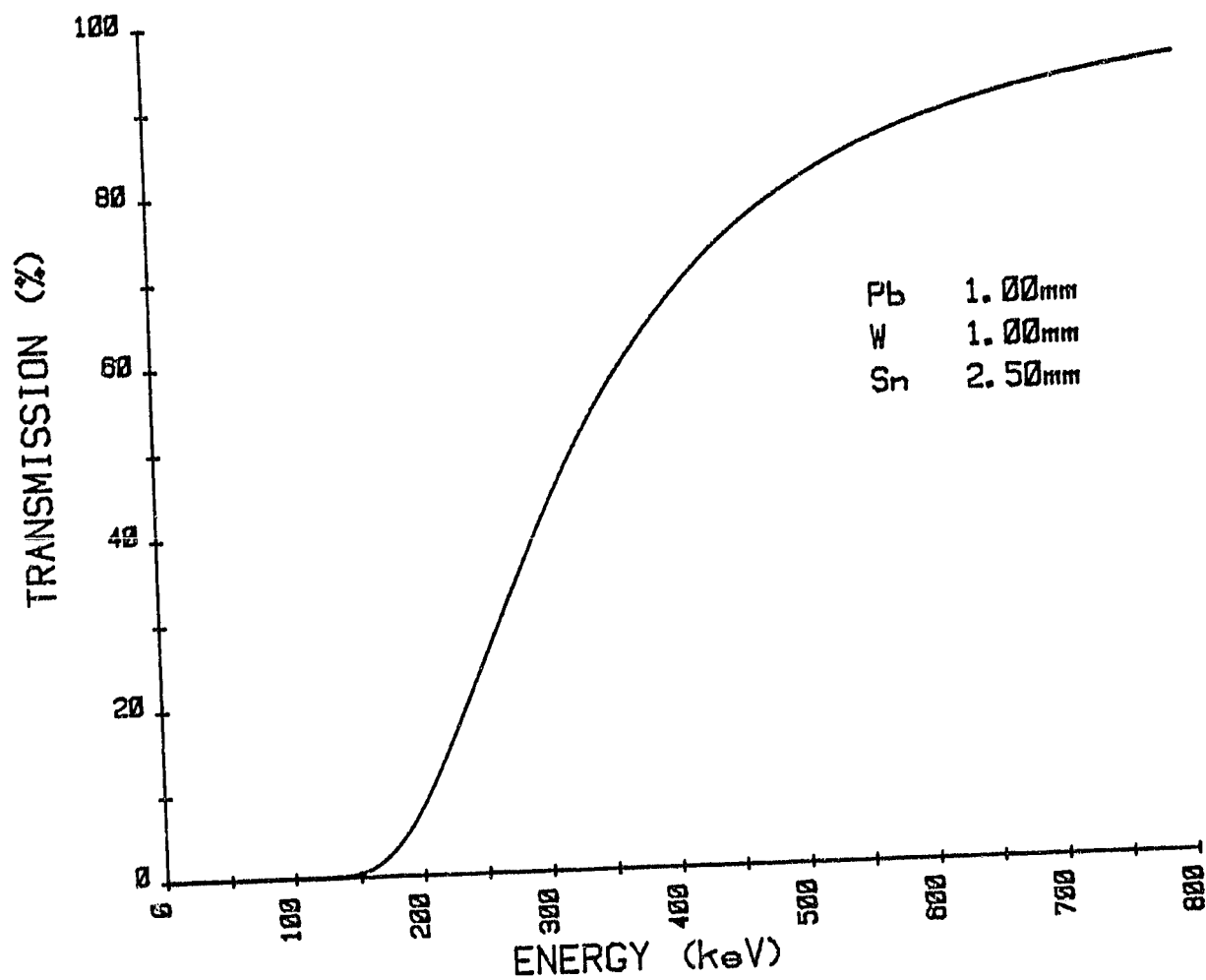
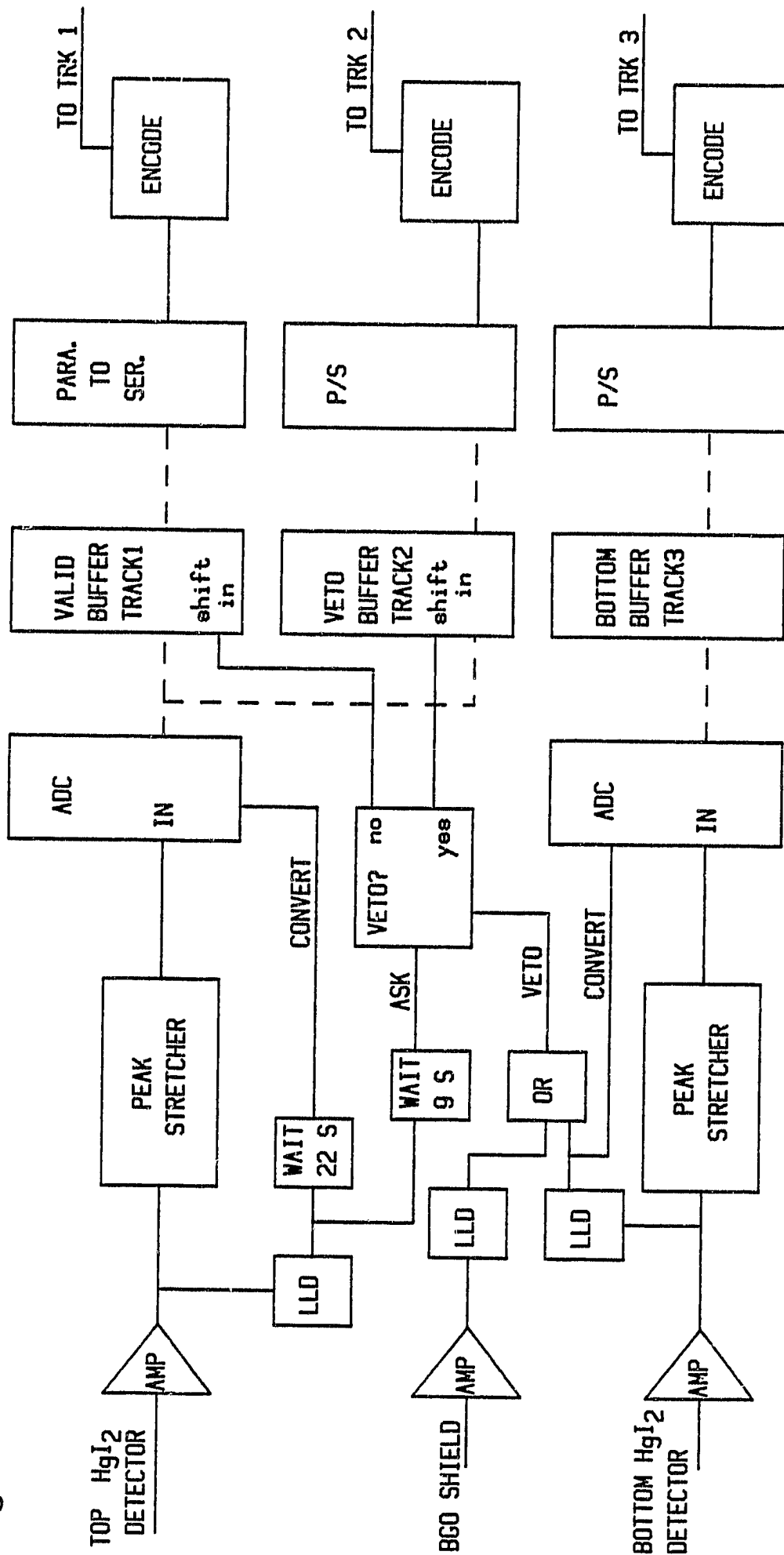


FIGURE 3

Figure 4 EVENT LOGIC DIAGRAM

--- 8 bit parallel data





ORIGINAL PAGE 13  
OF POOR QUALITY

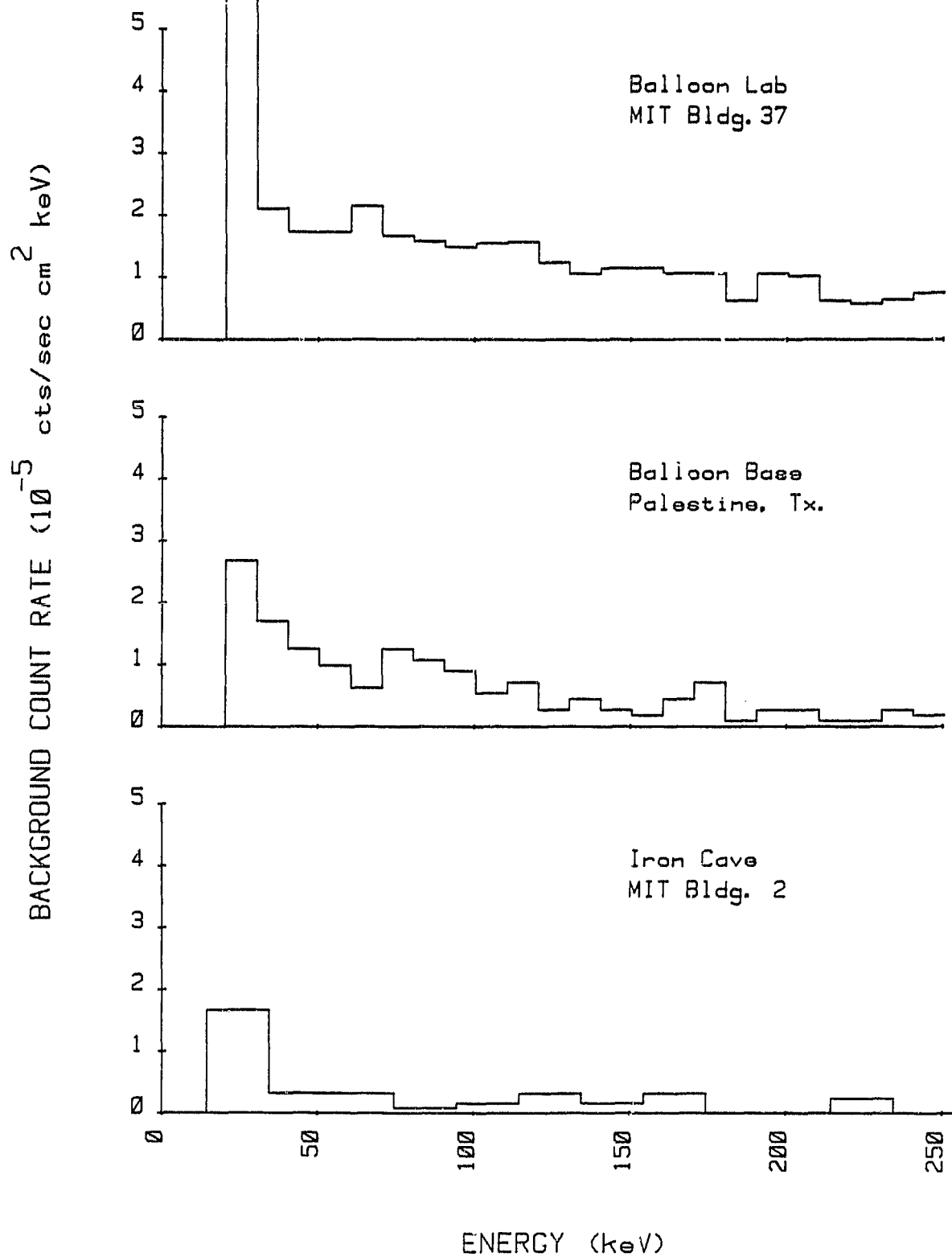


FIGURE 5

ORIGINAL PAGE 13  
OF POOR QUALITY

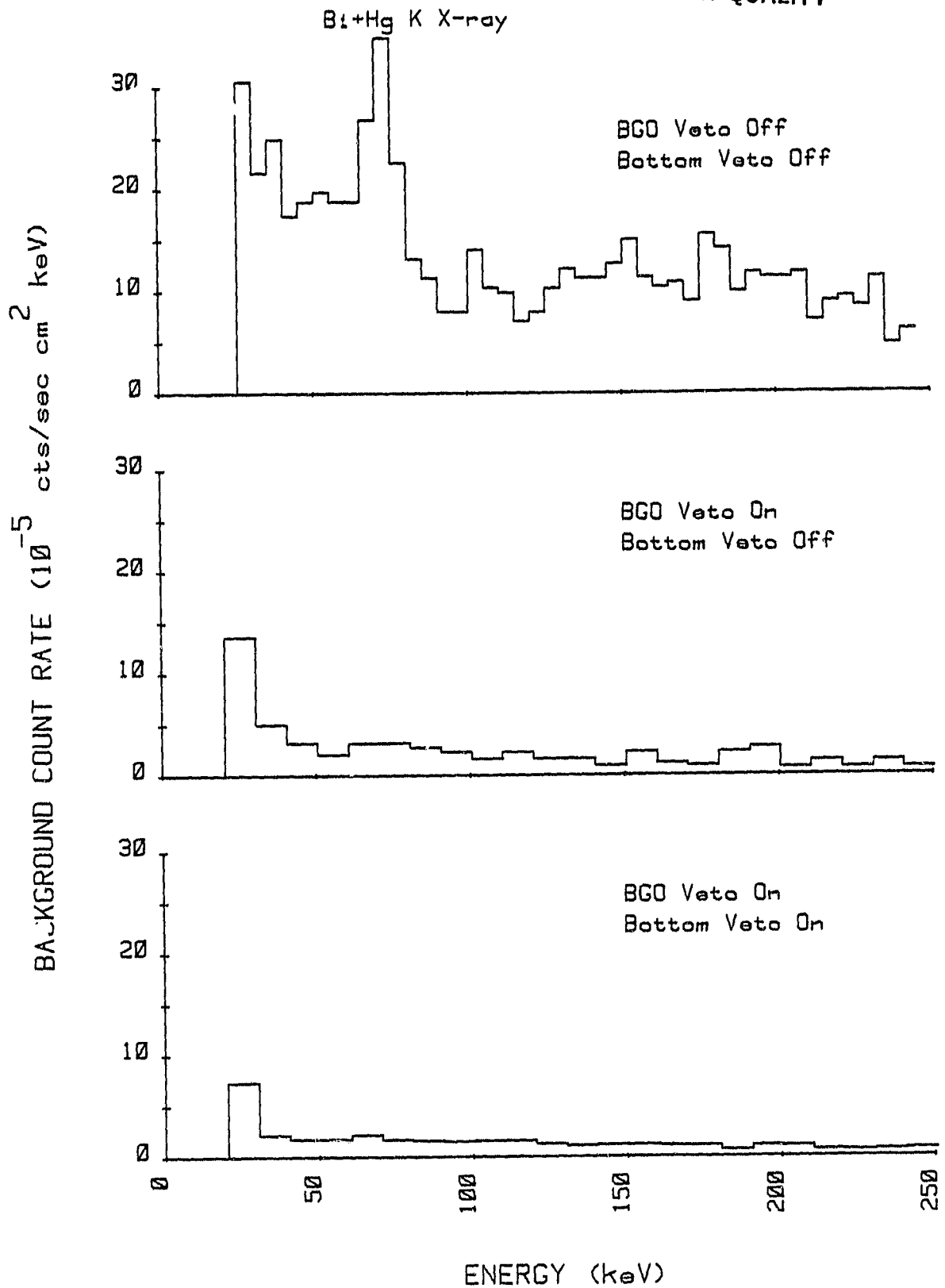


FIGURE 6

ORIGINAL PAGE IS  
OF POOR QUALITY

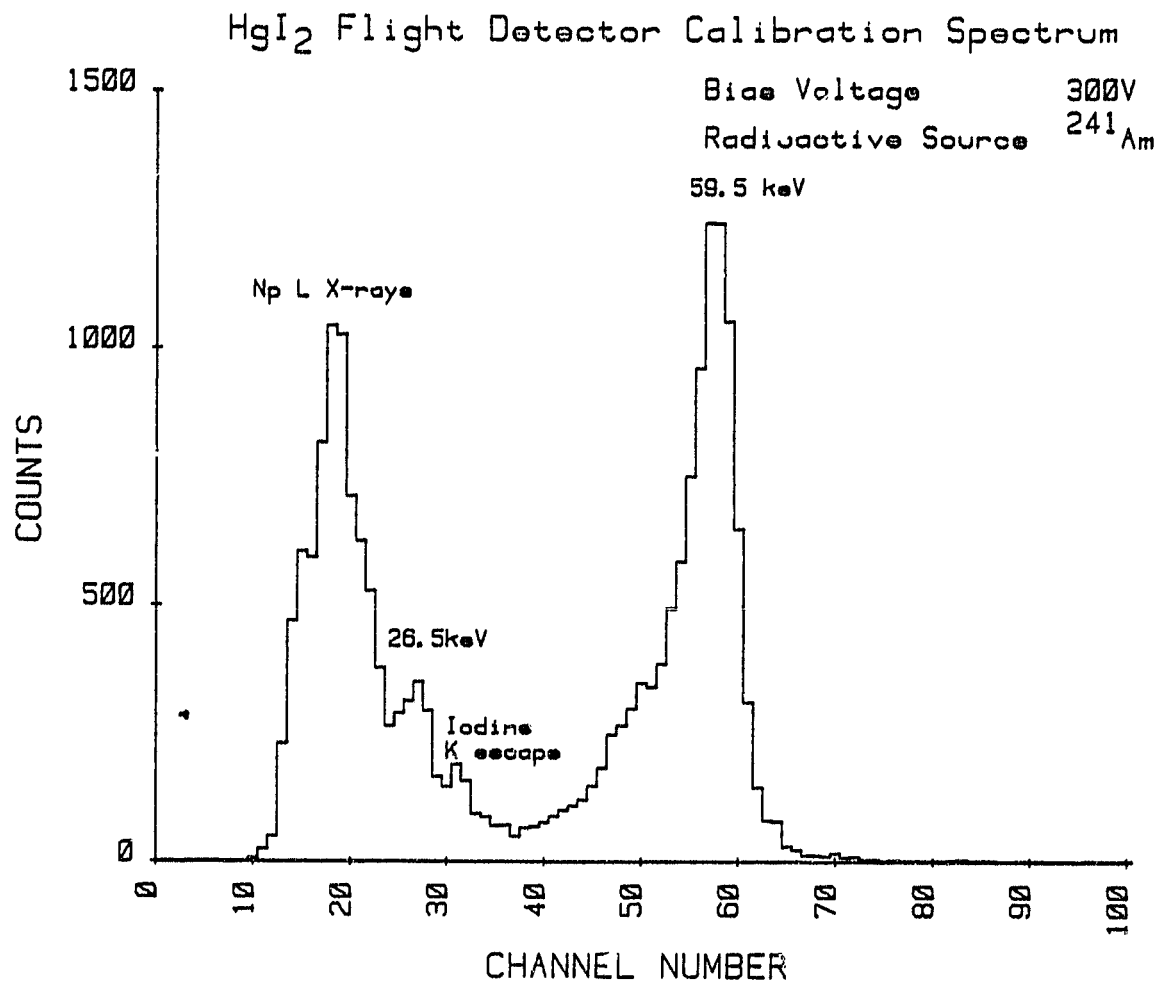


FIGURE 7

ORIGINAL PAGE 13  
OF POOR QUALITY

FLIGHT 1282P MAY 8, 1982

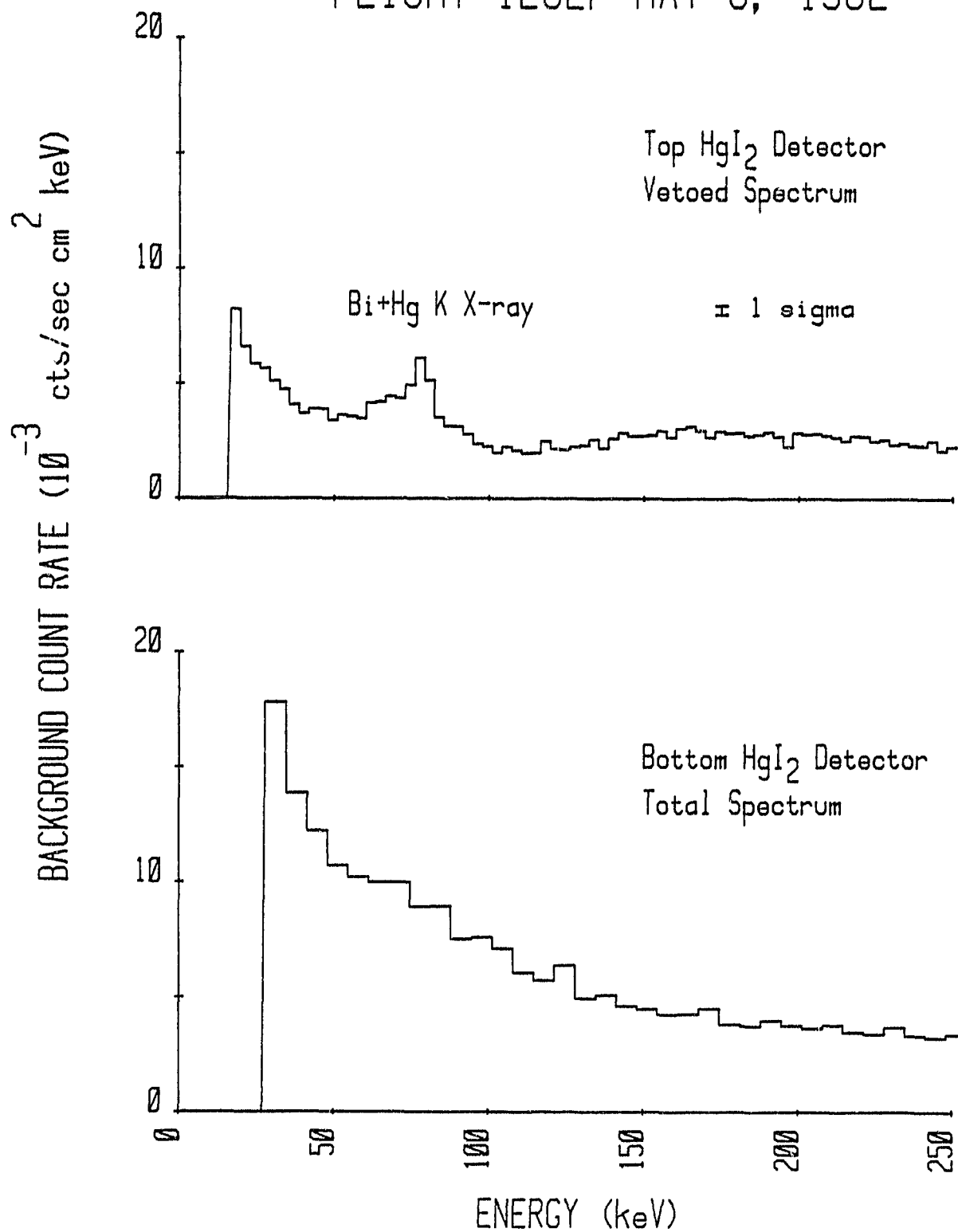


FIGURE 8

FLIGHT 1292P JUNE 21, 1982

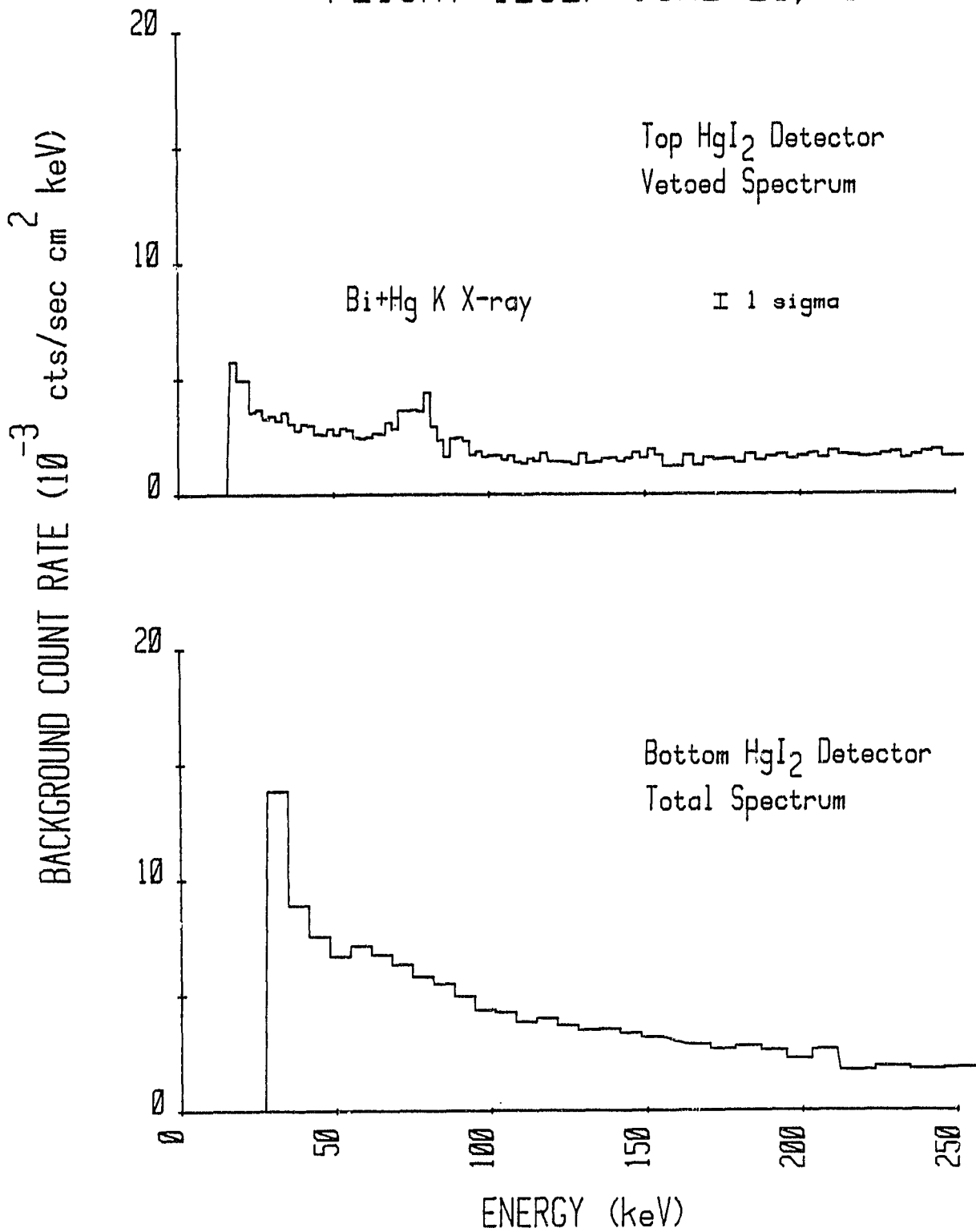


FIGURE 9

ORIGINAL PAGE 13  
OF POOR QUALITY

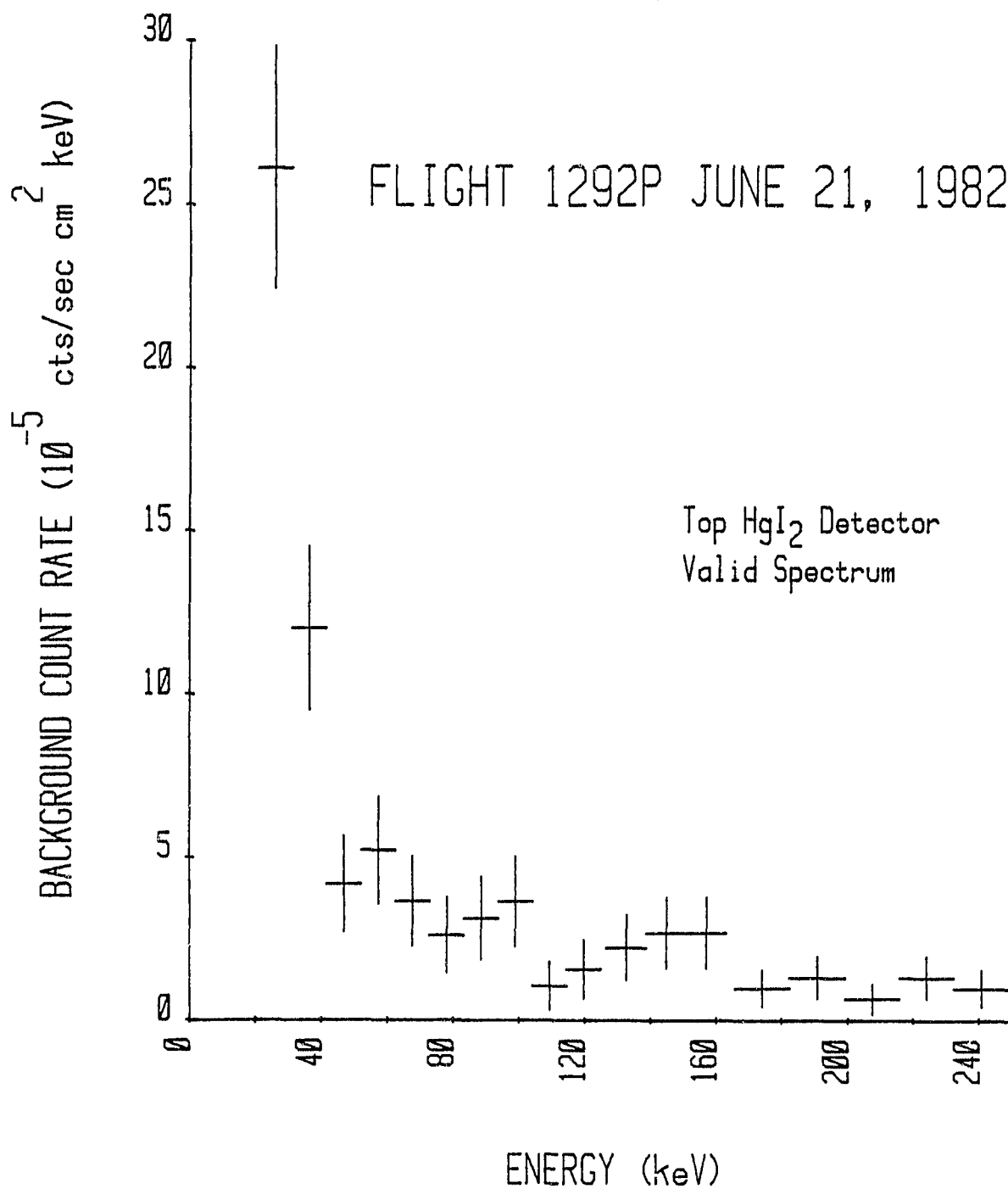


FIGURE 10

CPM 1.00E 13  
0.00E 00

## FLIGHT 1292P

INTEGRAL COUNT RATE VS. TIME  
Bottom Detector ( $E > 28\text{keV}$ )

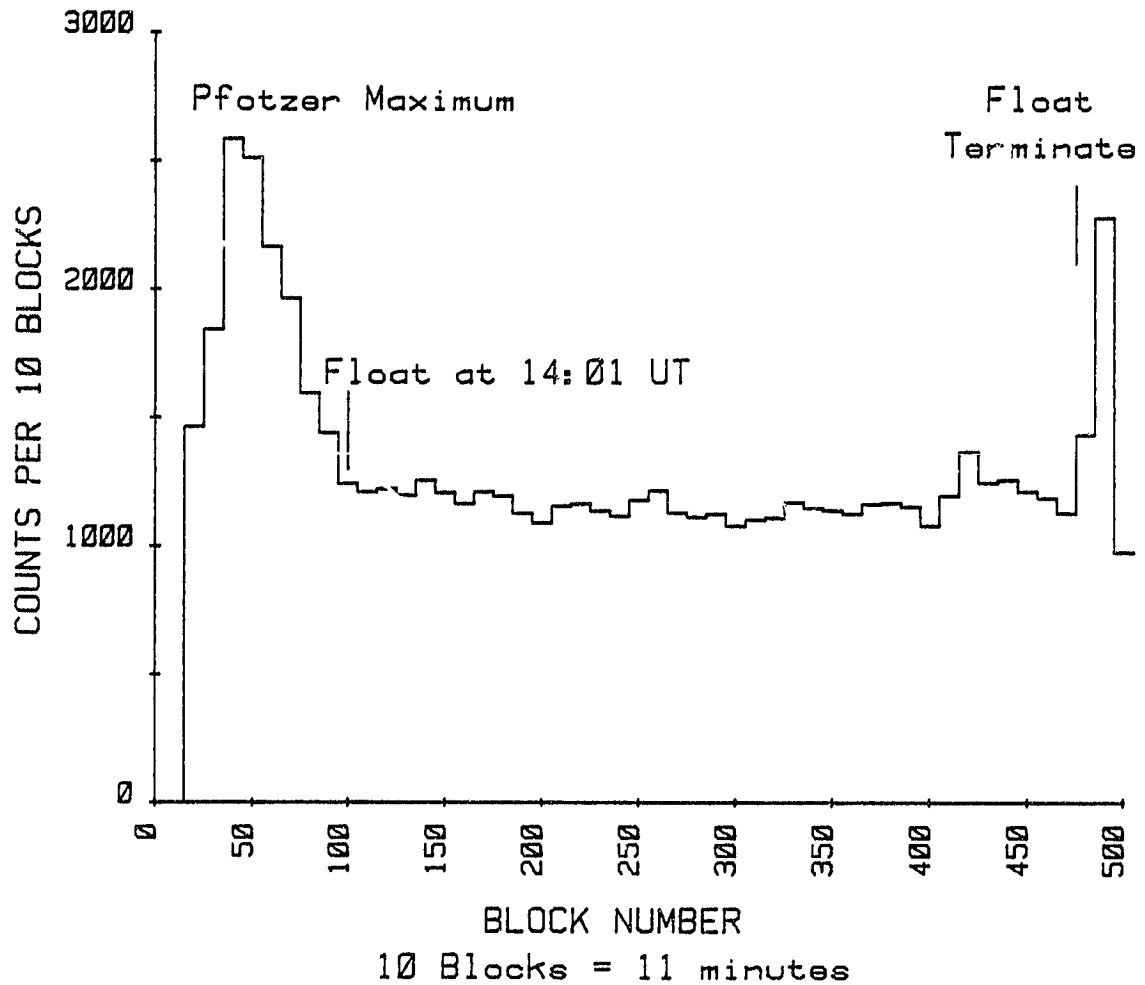


FIGURE 11